Solid State Science and Technology, Vol. 19, No2 (2011) 285-300
ISSN 0128-7389

DIELECTRIC PROPERTIES OF $B_2O_3 – TeO_2 – Sm_2O_3$ GLASSES SYSTEM

C. Zuraini, W.M.D.W. Yusoff , M.K. Halimah and A.W. Zaidan

Department of Physics, Faculty of Science, University Putra Malaysia, 43400 UPM Serdang, Selangor Darul Ehsan.

Corresponding author: iniaruz_s@yahoo.com

ABSTRACT

Glasses in the system containing $[B_2O_3]_{0.3}$ $[Te0_2]_{0.7-x}$ $[Sm_2O_3]_x$ was prepared from melt-quenching technique over a wide range of composition (x = 0.3~1.2 mol%) denoted as BTS1, BTS2, BTS3, BTS4 and BTS5 respectively. The structural changes were studied by XRD spectra, FTIR spectroscopy and DTA spectra. Network units existed in Sm^{3+} doped glass and Sm^{3+} existed as network modifier. The higher concentration of Sm^{3+}, the more units of TeO_3 would transform to TeO_4. The optimum Sm^{3+} concentration was about 1.0 mol% (BTS4) for this glasses system. The density (ρ) and molar volume (V_m) was obtained attributed to non-bridging oxygen (NBO). The addition of samarium oxide ($4f^5$) indicates of strong bonding between the components and enhances the glass formation ability. The dielectric properties (dielectric constant, ε', and dielectric loss factor, ε''), which were characterized in the frequency range 10^{-2} – 10^6 Hz over temperature range 100 – 220 ^oC, show a larger value at lower frequencies (below 100 Hz) and higher temperatures (above 140 ^oC). The graphs were fitted using Cole-Cole and Quasi dc models. Activation energy obtained from the master plot graph was found to decrease as Sm_2O_3 content increased. The optical band gap was found to decrease with increasing Sm_2O_3 content attributed to increase in degree of disorder in the system, direct consequence of the increases of NBO in the system.

Keywords: Dielectric Properties; $B_2O_3 – TeO_2 – Sm_2O_3$ glasses; Rare Earth; Polarization; Non-Bridging oxygen;

INTRODUCTION

Rare earth ions doped materials have broad band-region from ultraviolet to infrared, so these functional materials have been widely used in many fields, such as laser protection, nonlinear optical field, light communication and laser materials and also commonly used in the production of sunglass lenses. It has been ranked crucial elements by America, Japan etc., for developing high technology [1].

The dielectric properties of glass materials are an intrinsic effect associated to the mechanism of polarization of the permanent and induced electrically charges by an external applied electric field. The polarization contributions to the capacitance were attributed to the existence of degrees of freedom associated with permanent dipoles from the charge pairs comprised by the positive glass modifier ions and either

negatively charged non-bridging oxygen (NBO) or else by charged tetrahedral structural units [2]. Glass structure is a basic issue to better understanding the behavior of the materials. The structure of oxide glasses can be expressed by the kind and type of oxygen coordination polyhedral in the structure and the way they interconnect to each other to form the glass network. Influence of glass-modifier additions such as Sm_2O_3 effects on structural changes related to BO_4/BO_3 ratios have been extensively studied [3-5]. It has been proposed that in oxide glasses a rare earth ion is surrounded by eight neighbouring oxygen atoms belonging to the corners of BO_4-forming tetrahedral. Each tetrahedron donates two oxygen atoms forming an edge of the cube. It is assumed that the resulting glass is composed of both triangular and tetrahedral units, which form a relatively open network with holes between the oxygen atoms of sufficient size to accommodate the Li and Na or Li and K or Na and K ions [6].

Samarium ion with $4f^5$ electronic configuration usually exists in triply ionized (Sm^{3+}) state and its spectrum has been studied in solution as well as in solid phases by several workers [1, 3, 6-10]. Network units existed in Sm^{3+} doped glass and Sm^{3+} existed as network modifier [1, 3, 7]. These rare earth ions enter the glass network as modifiers by breaking up the random network, thereby leaving the NBO in the B_2O_3 glass lattice [8]. Among the various types of glasses, the tellurite based glasses exhibit high dielectric constant and electrical conductivity compared to other glass systems, which has been argued to be due to the unshared pair of electrons of the TeO_4 group that do not take part in the bonding [11]. TeO_2 is known as a conditional glass former, in the sense that it needs a modifier in order to form the glassy state easily [12]. Previous researcher [13, 14] state that, in tellurite glasses with high TeO_2 contents; the TeO_4 triangular bypiramid is the basic coordination polyhedron. In this configuration, tellurium atoms are surrounded by four oxygens each connected to two tellurium atoms, creating an axial equatorial bonding in which the bonds can easily be deformed. This changes in the Te-$_{ax}O_{eq}$-Te angle takes place along the C axis through the incorporation of the modifier (Sm_2O_3) [1] into the structure, which creates defects and oxygen vacancies, in which increases the number of NBO. In the glass structure, the rare earth ions have two functions; the first one is that samarium ions having high-field-strength will concentrate glass net structure which is the crystallization tendency of the glass is strengthened and the glass-forming ability of the rare earth doped glasses is weakened; the second one is that Sm_2O_3 acts as a network modifier which makes the number of the free oxygen increasing with the rare earth oxide added. With more rare earth oxide added, free oxygen ions increase, too. While the samarium oxide content increases excessively, this concentration effect of rare earth ions may intensify [9]. Nevertheless, according to Ni Yaru [1] and Akshaya [7]; with the increment of Sm^{3+} ions, the distance between the rare earth ions would be shortened, and the dipole-quadrapole interaction would be enhanced between Sm^{3+} ions, in which resulted in Sm^{3+} concentration quenching.

The present study is a report characterizing Sm_2O_3 concerning the composition, structural, optical and dielectric properties as a function of frequency and temperature. The present investigation on the dielectric properties may be useful to understand the mechanism of the polarization process. Also, we try to get the parameters necessary for

the basic understanding of the physical grounds of optical properties.

EXPERIMENTAL DETAILS

The chemical composition of the tellurite glass doped with different concentrations of Sm^{3+} used in the present studies is as follows:

$$[B_2O_3]_{0.3}\ [Te0_2]_{0.7-x}\ [Sm_2O_3]_x$$

where the quantities are taken in mol% and x = 0.3, 0.5, 0.7, 1.0 and 1.2 mol%, prepared by melt-quenched technique. The starting chemical used were Analar grade quality with Sm_2O_3 (99.9% purity), TeO_2 (99% purity) and B_2O_3 (97.5% purity). These chemical powders being weight accurately and mixed thoroughly. The batches were placed in alumina crucibles and melt in electrical furnace at their glass forming temperature (1000 ^oC) for an hour. The glass molten was then poured into stainless steel cylindrical shaped split mould which had been preheated at 300 ^oC. The sample was later placed into the annealing furnace at temperature 300 ^oC for 2 hour. After that, the furnace be shutdown and quenched to room temperature. The prepared glass samples were free from bubbles and have a light yellow color coming from the Sm^{3+} f-f transitions. The samples will be cut and polished into desired dimensions (thickness 2 mm) and later were coating with aluminium foil to serve as electrode for dielectric measurement. The excess prepared samples were ground into powder form for XRD, FTIR and DTA measurements. The glassy state of the system was conducted by X-ray diffraction measurement using X'pert Pro Panalytical, in which no crystalline phases were observed. The IR spectra were recorded using Fourier Transform Infrared Spectroscopy (FTIR) in the frequency range 280 - 4000 cm^{-1} at room temperature. The density of the samples was determined by the usual Archimedean method (involving weighing in air and in water as the reference liquid) and the molar volumes were calculated. The differential thermal analysis (DTA) measurements were recorded to provide data on the transformations that have occurred, such as glass transitions. The electrical measurement (dielectric constant ε', dielectric loss factor ε'') were characterized in the temperature range of 100 – 220 ^oC over frequency range of 10^{-2} – 10^6 Hz using High Dielectric Resolution Analyzer (Novo-control). The graph fitted using superposition of Cole-Cole functions in addition to Quasi-dc terms. The activation energy was calculated corresponding to master curve fitting and the optical absorption was utilized at room temperature in the wavelength range of 190 – 1100 nm using UV-VIS-Shimadzu double beam spectrophotometer.

RESULTS AND DISCUSSION

Infrared (IR) spectra

Representative spectra of the glasses studied are shown in Figure 1. Increasing the Sm_20_3 content of the studied glasses generates: (i) the shift band from 319~320 cm^{-1} was assigned as the presence of Samarium oxide, in which Sm is well-known metal oxides. Optimum concentrations were found at 1.0 mol% (BTS4) [1, 7]. The intensity increased, near the 320 cm^{-1} band with increasing concentration of Sm_20_3 up to BTS4

and then the intensity decrease. This may be due to incorporation of the modifier into the network of glass-former. As a result of the degree of covalency present leads to broadening of the IR bands [12, 14], (ii) the shift band from 646~675 cm^{-1} was attributed to the Te-O-Te bridges between four coordinate tellurium atoms [TeO_4]. The intensity of the latter is found to increase with increasing Sm content, (iii) the shift band from 846~820 cm^{-1} was assigned to the B-O-B bending vibrations, Te-O bending vibrations in [TeO_3]. The spectra show that the latter broad band is sensitive to the samarium content; its intensity decreases with increasing samarium oxide concentration. This is due to the increase in the number of TeO_4 bonds, since the addition of samarium oxide is at the expense of Sm_20_3 and TeO_2, (iv) the shift band from 1235~1225 cm^{-1} was attributed to the B-O stretching vibrations in [BO_3] units from boroxol rings. The position of this band is found to be almost independent of Sm content up to BTS4, and (v) the shift band from 1360~1365 cm^{-1} and the increase of intensity was assigned to the vibrations of the [BO_3] units from varied types of borate groups.

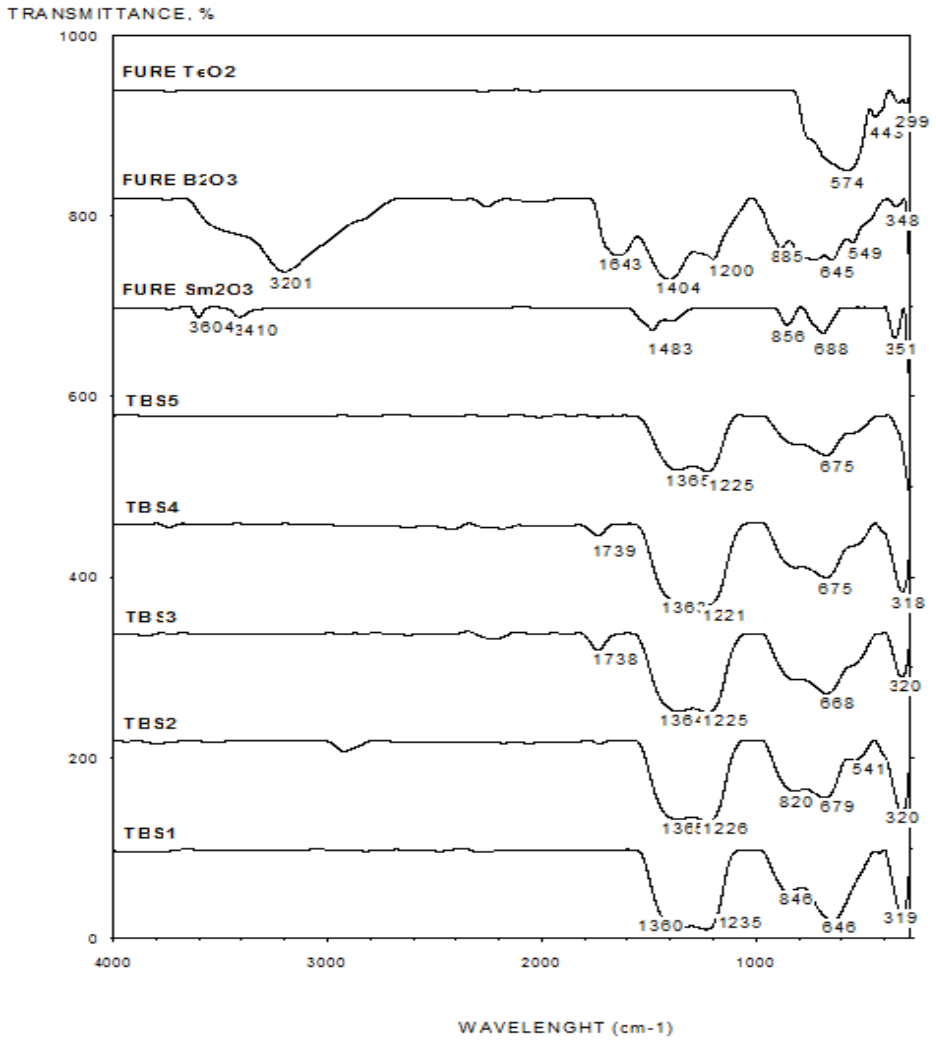

Figure 1: The FTIR spectra of $[B_2O_3]_{0.3}$ $[Te0_2]_{0.7-x}$ $[Sm_2O_3]_x$ glasses system

Taking into account these changes of the IR spectral features, we assume that the increase of samarium oxide up to BTS4 (1.0 mol%) in the glass structure leads to the following: (i) the number of the [TeO_4] groups with non-bridging oxygens increase because some trigonal pyramidal [TeO_3] structural units were transformed in trigonal bipyramidal [TeO_4] units and (ii) the disintegration of some boroxol units and the transformation of some tetrahedral [BO_4] units into trigonal [BO_3] units [4, 13, 14, 16].

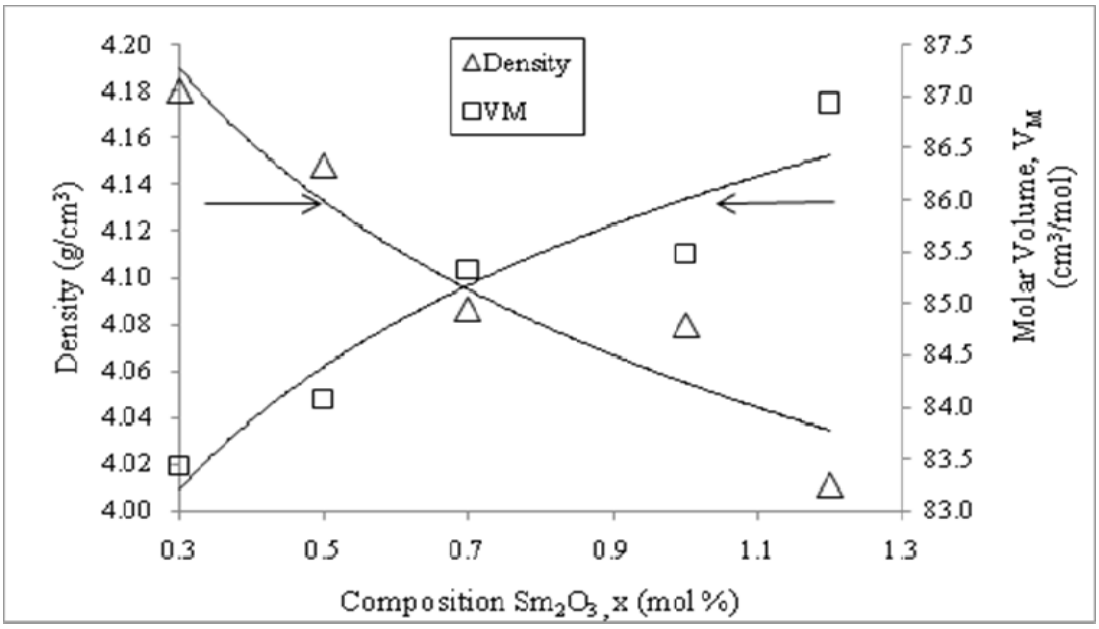

Figure 2: Composition dependence of density (g/cm^3) and Molar Volume, V_M (cm^3/mol) for $[B_2O_3]_{0.3}$ $[Te0_2]_{0.7-x}$ $[Sm_2O_3]_x$ glasses system

Density and Molar Volume measurements

Figure 2 illustrates the density and molar volume of the investigated samples as a function of Sm_20_3 mole fraction. The values obtained were shown in Table 1. It is clear that the density decreases linearly with increasing samarium oxide mole fraction up to BTS4. This decrement is most likely may attribute to increasing of non-bridging oxygen and decrease of bridging as can be seen in IR discussion part [3, 13]. In such systems the number of the [TeO_4] groups with non-bridging oxygens increase because some trigonal pyramidal [TeO_3] structural units were transformed in trigonal bipyramidal [TeO_4] units. It is also known that, B_2O_3 in its glassy form is a laminar network consisting of boron atoms three-fold coordinated with oxygen. Upon modification with a rare earth oxide, the taken off oxygen, losing by the oxide dissociation, causes an association transformation of BO_4 coordination into BO_3 coordination (proven in IR spectra). The number of BO_3 unit increases thus these units increase the number of NBO and are responsible for the decrease in the connectivity of the glass network. As a result, the degree of the structural compactness would decrease which leads to decrease in density, i.e. the density of the glasses depends on the compactness of the structural units [3-5, 9, 17]. At high concentration (above BTS4), the density increases assigned as

Sm^{3+} concentration quenching [1, 7] in which the connectivity of tellurite network increases, i.e. bridging oxygen formed [1, 18]. Generally, the behaviour of molar volume follows a trend opposite to that of density which is the normal expected behaviour. Molar volumes were found to be increase with an increase in Sm_2O_3 content up to BTS4. As a result of the creation of NBO, which break the bond tellurite borate host glass, will increased the distances between structural groups of the studied glasses system. The larger the values of ionic radii between them will increase the overall molar volume of these glasses [18].

Table 1: Density, ρ and Molar Volume, V_M for $[B_2O_3]_{0.3}$ $[Te0_2]_{0.7-x}$ $[Sm_2O_3]_x$ glasses system

Glasses	ρ (g/cm^3)	V_M (cm^3/mol)
BTS1	4.18	83.43
BTS2	4.15	84.07
BTS3	4.09	85.32
BTS4	4.08	85.47
BTS5	4.31	80.88

DTA measurements

Figure 3 shows the glass transition temperature, Tg plots obtained from DTA spectra analysis for all glasses studied. The glass transition temperature Tg are listed in Table 2. It is clear that the Tg are increase with increasing in Sm_2O_3 content. The addition of elements Sm^{3+} ($4f^5$) which has a valency of 5, helps to reinforce an ordered lattice, and thus increases the Tg. This indicates strong bonding between the components. Thermal stability of glass depends on ΔT which is increased as Sm_2O_3 increases. In other words, the addition of Samarium enhances the glass formation ability [10, 12].

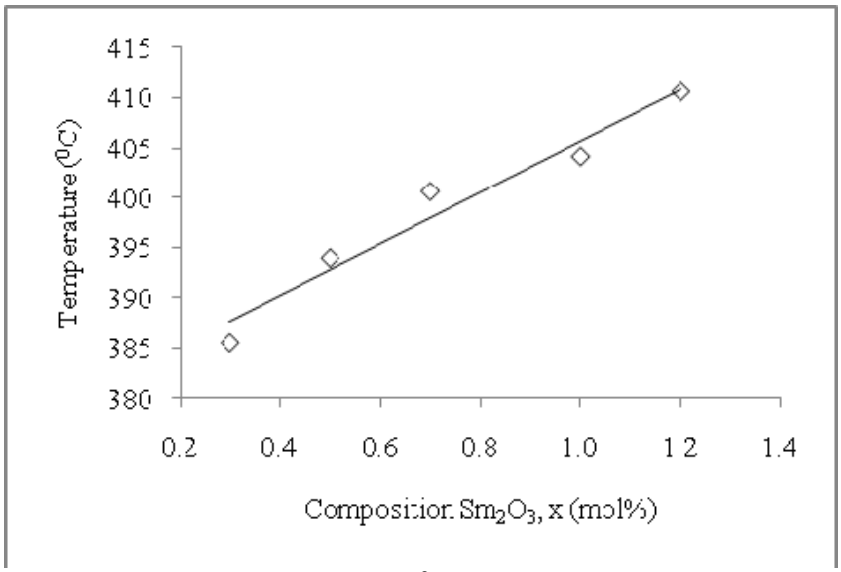

Figure 3: Glass transition temperature, Tg (^oC) at different Sm_2O_3 content for $[B_2O_3]_{0.3}$ $[Te0_2]_{0.7-x}$ $[Sm_2O_3]_x$ glasses system

Table 2: Transition temperature, T_g and Crystallization Temperature, Tc for $[B_2O_3]_{0.3}$ $[Te0_2]_{0.7-x}$ $[Sm_2O_3]_x$ glasses system

Glasses	T_g (^{0}C)	Tc (^{0}C)	$\Delta T = Tc - T_g$
BTS1	385.606	490.456	104.85
BTS2	393.968	489.086	95.118
BTS3	400.617	481.098	80.481
BTS4	404.244	480.054	75.810
BTS5	410.723	477.182	66.459

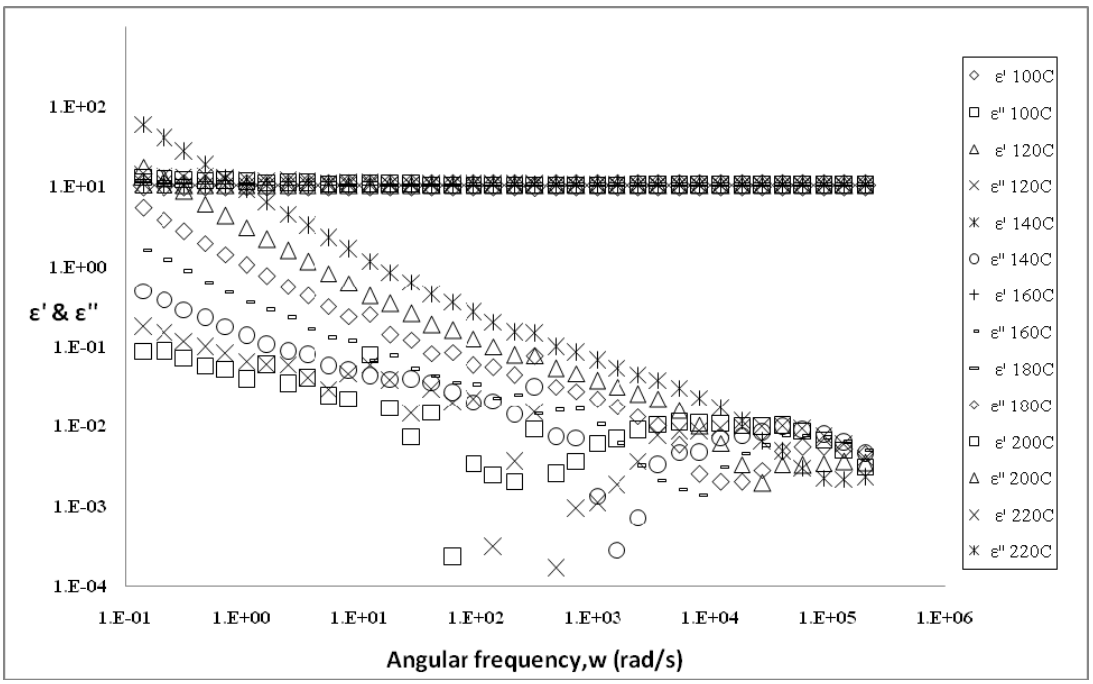

Figure 4: Variation of dielectric constant (ε') and dielectric loss factor (ε'') with frequency at temperature 100 – 220 ^{o}C for BTS1

Electrical measurements

Frequency dependence of the dielectric properties

The plot of dielectric constant (ε') and dielectric loss factor (ε'') with frequency illustrated for glass BTS1 at various temperatures is shown in Figure 4. From Figure 4, the ε' decrease with increase in frequency. The features can be explained by the fact that at low frequencies the electronic, ionic, dipolar and interfacial/surface polarizations contribute to the dielectric permittivity. The contributions of the interfacial polarizations occur at frequency below 100 Hz, after that the values of ε' become frequency-dependent. The interfacial polarization can be explained using a Maxwell-Wagner mechanism, which is concerned due to ionic motion in the presence of an electric field.

At low frequencies (below 100 Hz) the mobile charges, usually impurity ions diffuse under the influence of the applied electric field up to the interface and build up the surface charge until the applied field reverse with the alternating voltage. The ionic motions are sensitive to the frequency of the alternating field and cannot follow the field variations at very high frequency (above 100 Hz) [15, 16]. This effect can also be seen in variation of dielectric loss factor (ε'') with frequency for BTS1 shown in Figure 4. From this figure, i.e. shows that ε'' decrease with increase in frequency due to the interfacial polarizations concerned to ionic motions which is sensitive to the frequency of the alternating field and cannot follow the field variations at very high frequency; same behavior was observed in ε'.

Temperature dependence of the dielectric properties

Figure 5(a) and Figure 5(b) shows that the variation of dielectric constant (ε') and dielectric loss factor (ε'') in the temperature range 100 – 220 ^{o}C. The ε' and ε'' has a very low values and remains almost constant up to 140 ^{o}C (413 K) and thereafter it increases rapidly with temperatures. The rapid increase of ε'' at higher temperature (above 140 ^{o}C) in the low-frequency region may be due to space charge polarization, which can be explained using the Shockley-Read mechanism. For low and middle-order frequencies and at high temperatures the impurity ions in the bulk crystal matrices capture the surface electron, causing the space-charge polarization at the surface. The surface electron capture process increases with increase in temperature. Due to this mechanism, the dielectric loss factor (ε'') increase with increasing in temperature in the high temperature region (at low frequency). Same behavior was observed in ε' [8, 15, 16].

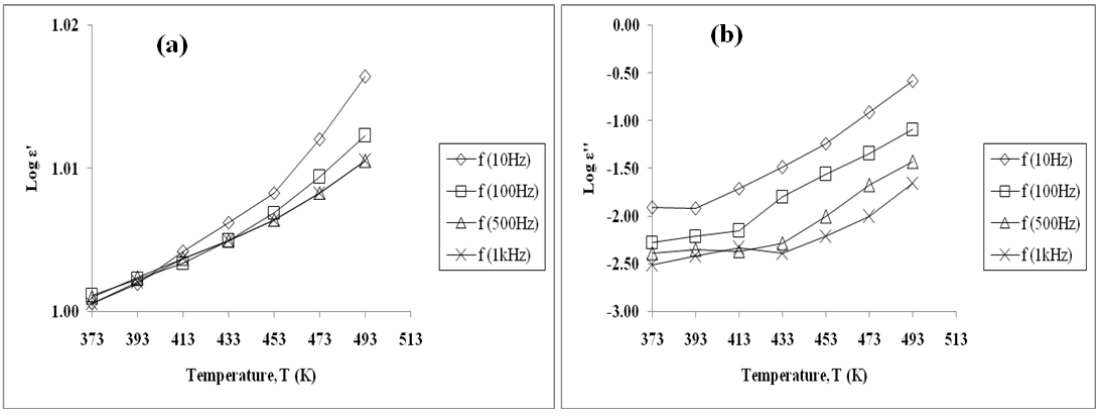

Figure 5: Temperature variation at certain frequency for BTS1; (a) Dielectric constant, ε', (b) Dielectric loss factor, ε''

Fitting Models of the dielectric properties

From Figure 4, the curves relating (ε'') with frequency shows that more than one relaxation process is present. With all the different spectral functions commonly used in dielectric research for instance Debye, Cole-Cole, Cole-Davidson and Havriliak-

Nagami, the data of BTS1 at 220 ^{0}C was fitted and the best fitting of the data was contribute by a superposition of Quasi-dc functions and Cole-Cole functions.
The spectral function expressed as:

$$\varepsilon_r(\omega) = \varepsilon^*(\omega)_{QDC} + \varepsilon^*(\omega)_{C-C} \tag{1}$$

has been used to analytically represent the measured spectra. The $\varepsilon_r(\omega)_{QDC}$ denotes as Quasi-dc function form, $\varepsilon_r(\omega)_{C\text{-}C}$ denotes as Cole-Cole function.
Both function represented as:

$$\varepsilon^*(\omega)_{QDC} = A(i\omega)^{-p} + B(i\omega)^{n-1} \;\; ; 0 \le p, n \le 1 \tag{2}$$

where p and n are constant for a given material.

$$\varepsilon^*(\omega)_{C-C} = \varepsilon_\infty + \frac{\varepsilon_s - \varepsilon_\infty}{1 + (i\omega\tau_{C-C})^{1-\alpha}} \;\; ; 0 \le \alpha \le 1 \tag{3}$$

where $\tau_{C\text{-}C}$ is the mean relaxation time and α is a constant for a given material, having a value of $0 \le \alpha \le 1$. ε_s is the static permittivity and the ε_∞ is permittivity at infinite frequency.

Illustrated example of the dielectric spectrum and the fitting of the BTS1 at 220 ^{o}C are shown in Figure 6(a) and Figure 6(b), in which it clearly shows that the theoretical values are in good agreement with the experimental ones. The dielectric behavior at low frequency shows a quasi dc behavior quoted as low frequency dispersion (LFD) behavior. The value of p lies in between 0.8 to 0.9 and the values of n lies in ranges from 0.94 to 0.98. Based on the Dissado-Hill theory, the cluster model for dielectric relaxation may be due to two kinds of displacement fluctuations, which is inter-cluster (between adjacent clusters) or intra-cluster motion (within a cluster). The inter-cluster motion (at low frequency branch) has larger range than the intra-cluster motion (at high frequency branch spectra), in which result the quasi dc behavior of low frequency dispersion (LFD) spectra. The larger value of n indicates that electrons motion in the sample is strongly correlated between clusters [19].

The Cole-Cole relaxation parameters α lies in between 0.2 to 0.3 for all temperature studied. The value of α leads to a decrease value when the temperature were further increased. These low-frequency losses may be due to Shockley-Read losses assigned as the space charge polarization caused by the impurity ions of the investigated systems [20].

According to the spectral function expressed in equation (1), the best dielectric data of all studied sample were fitted and we assume to propose the model shows in Figure 7 due to superposition of Cole-Cole functions and Quasi-dc functions.

Solid State Science and Technology, Vol. 19, No2 (2011) 285-300
ISSN 0128-7389

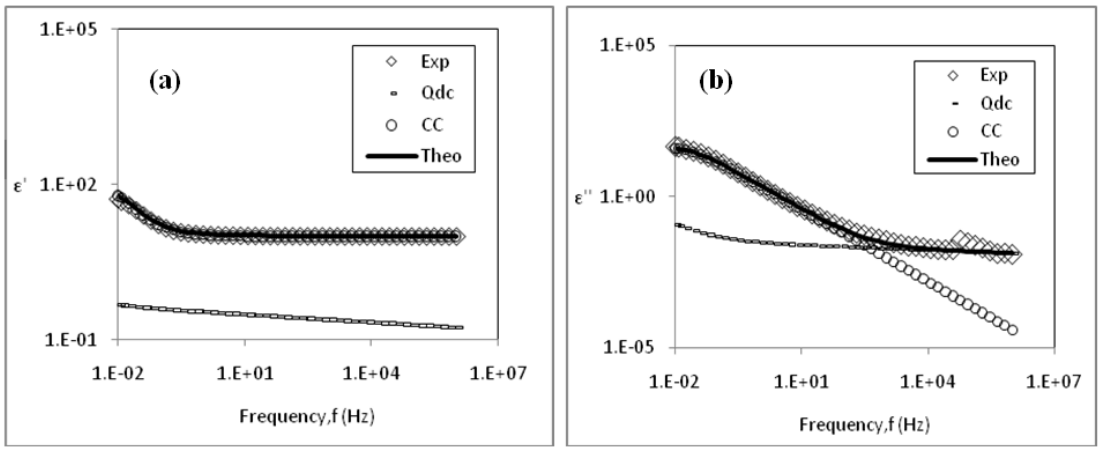

Figure 6: Plots of experimental and theoretical value at 220 ^{o}C for BTS1; (a) Dielectric constant, ε', (b) Dielectric loss factor, ε''. Both data fitted by Qdc (····), Cole-Cole (oooo), Experimental data (◇◇◇), and Total fit (——).

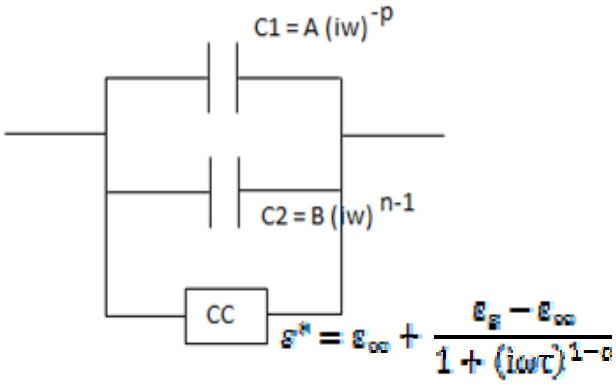

Figure 7: The proposed model obtained due to the fitting models

Activation energy, E_a

The activation energy, E_a obtained from correlated master curve in all frequency range and temperature range illustrated by BTS1 sample shows in Figure 8. Plots of Ln f against 1000/T (K^{-1}) were represented in Figure 8 (inserted) and yielded a straight line for all glasses by fitted an equation of the form [21]:

$$f = f_0 \exp\left(-\frac{E_a}{kT}\right) \qquad (4)$$

where f_0 and E_a are the attempt frequency and the activation energy, respectively. E_a are constants determined from the intercept, the slope of the lines and k is Boltzmann constant.

Solid State Science and Technology, Vol. 19, No2 (2011) 285-300
ISSN 0128-7389

The E_a value obtained is decrease from 1.102 eV to 0.932 eV with increasing Sm_2O_3 content up to BTS4. Further increase of Sm_2O_3 content leads to increase in E_a from 1.088 eV to 1.089 eV. Those results may be due to the samarium oxide substance that modifies the transition state to lowers the activation energy. With samarium oxide as dopant in the system up to BTS4, the energy required to enter transition state decreases, thereby decreasing the energy required (E_a) to initiate the reaction. At high concentration, the Sm_2O_3 act as modifier without entering into glass matrix, so the value of E_a required to initiates the reaction becomes increased.

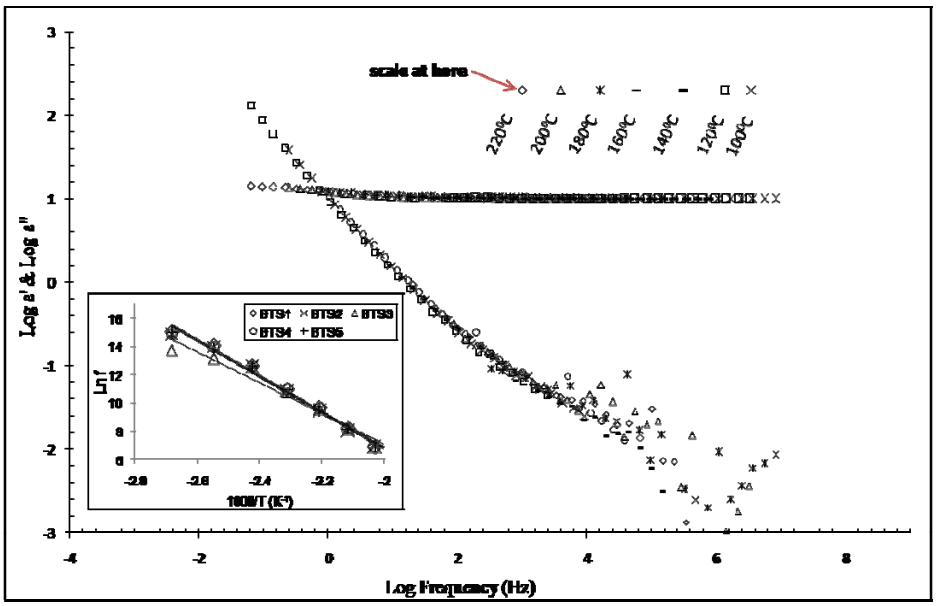

Figure 8: Master curve of sample BTS1 at temperature range 100 – 220 ^oC and frequency range 10^{-2} – 10^6 Hz. Inserted figure shows the plot of Ln f with 1000/T (K^{-1}) for all glasses sample

Optical band gap and Urbach Edge

Figure 9 illustrated the absorption spectra of B_2O_3 – TeO_2 – Sm_2O_3 systems. The data for Figure 10(a) and Figure 10(b) was obtained from the following relationship:

$$\alpha(\omega) = \frac{A(\hbar\omega - E_{opt})^n}{\hbar\omega} \qquad (5)$$

Where A is a constant, E_{opt} is the optical band gap, ħω is the photon energy and n is a constant which determines type of the optical transition. The values n = 2 and ½ correspond to direct and indirect transitions, respectively. Direct and indirect transitions, both of this involve interaction of an electromagnetic wave with an electron in the valence band (VB), by which the electron is then raised across the fundamental

gap to the conduction band (CB). The main factors contributing to edge broadening in materials are exciton–phonon coupling and the static structural disorders which contribute mainly to the absorption below the direct band gap and indirect band gap [22]. In order to see whether optical data on the present glasses fit better to the direct or indirect band gap formula; data $(\alpha\hbar\omega)^2$ versus $\hbar\omega$ as well as $(\alpha\hbar\omega)^{1/2}$ versus $\hbar\omega$ are plotted in the absorption region as shown in Figure 10(a) and Figure 10(b), respectively.

Direct or indirect energy band gap is determined from the linear regions of the plots as shown in the figures and corresponding values were shows in Table 3. The results show that the direct band gap has larger values than these indirect band gap and both values are decreasing with increase of Sm_2O_3 content up to BTS4. This result suggests that the covalent nature of the glass matrix decreases with increase of Sm_2O_3 concentration [17, 23, 24].

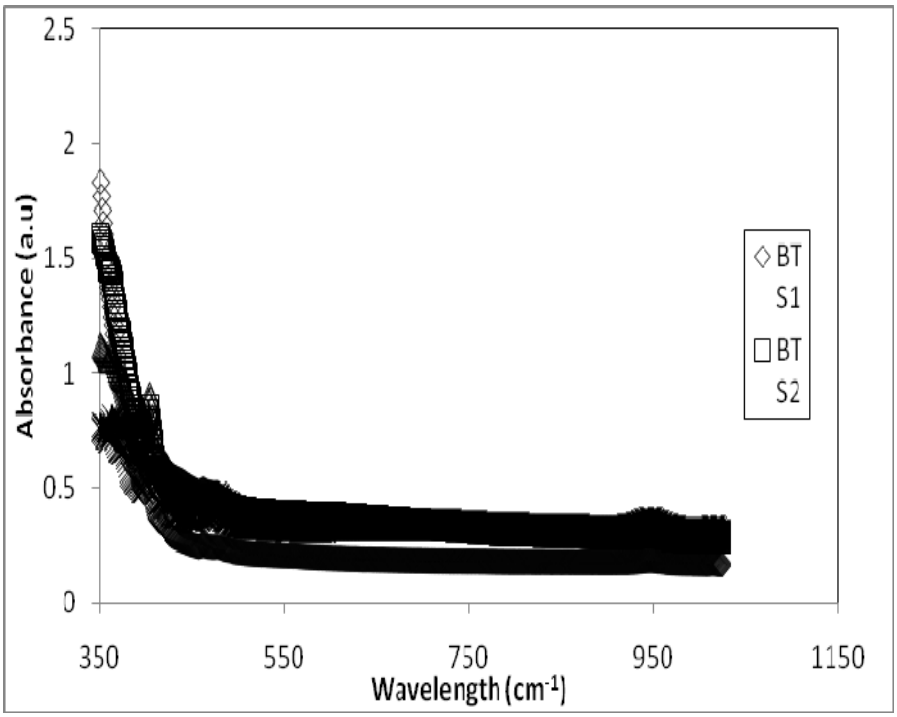

Figure 9: Optical absorption spectra of $[B_2O_3]_{0.3}$ $[TeO_2]_{0.7-x}$ $[Sm_2O_3]_x$ glasses system

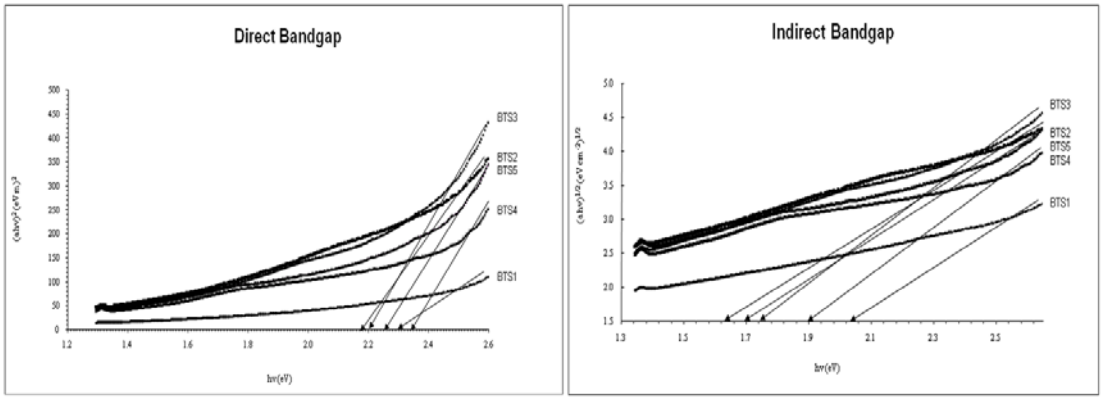

Figure 10: (a) Plot of $(\alpha\hbar\omega)^2$ against photon energy $\hbar\omega$ for direct band gap measurement, (b) Plot of $(\alpha\hbar\omega)^{1/2}$ against photon energy $\hbar\omega$ for indirect band gap measurement

Table 3: Direct optical band gap (E^1_{opt}), indirect optical band gap (E^2_{opt}) and Urbach energy (ΔE) of $[B_2O_3]_{0.3}$ $[Te0_2]_{0.7-x}$ $[Sm_2O_3]_x$ glasses system

Glasses	E^1_{opt} (eV)	E^2_{opt} (eV)	ΔE (eV)
BTS1	2.24	2.40	0.52
BTS2	2.12	1.64	0.71
BTS3	2.15	1.74	0.94
BTS4	2.26	1.90	1.15
BTS5	2.20	1.70	1.30

The fundamental absorption edge usually follows the Urbach Rule: [17, 23],

$$\alpha(\omega) = B\exp\left[\frac{\hbar\omega}{\Delta E}\right] \tag{6}$$

Where, B is a constant, ΔE is a measure of the band tailing and is known as Urbach Energy ΔE. The values of ΔE were calculated by taking the reciprocals of the slopes of the linear portion of the $\ln\alpha(\omega)$ versus $\hbar\omega$ curves in the lower photon energy regions as shown in Figure 11. These values are also included in Table 3. So, due to light doping, the band tailing or impurity band becomes broader and finally reaches and merges the bottom of the conduction band causing sudden decrease of the optical band gap [17, 23, 24].

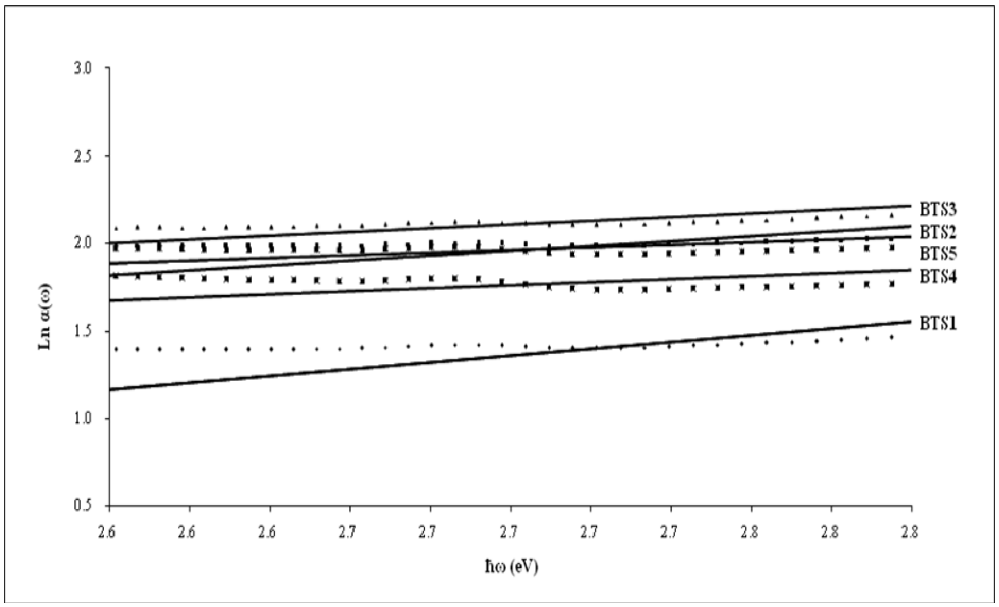

Figure 11: Optical absorption coefficient against photon energy ħω for $[B_2O_3]_{0.3}$ $[Te0_2]_{0.7-x}$ $[Sm_2O_3]_x$ glasses system

CONCLUSION

Based on the structural study Sm^{3+} existed as network modifier in $[B_2O_3]_{0.3}$ $[Te0_2]_{0.7-x}$ $[Sm_2O_3]_x$ glasses system. In conclusion, the optimum Sm^{3+} concentration was about 1.0 mol% (BTS4) for this glasses system. The dielectric properties (dielectric constant, ε', and dielectric loss factor, ε'') of this glasses system decreases with increase in frequency and also increases with increasing in temperature. It shows large dispersion at lower frequency (below 100 Hz) and at higher temperature (above 140 ^oC). At low frequency (below 100 Hz) the contributions of interfacial polarization can be explained using a Maxwell-Wagner mechanism [10, 16]. Whereas at higher temperature (above 140 ^oC) in the low-frequency region, may be due to contributions of the space charge polarization, in which can be explained using the Shockley-Read mechanism [8, 10, 16]. The proposed fitting model results from superposition of Cole-Cole functions and Quasi-dc denoted as LFD (low frequency dispersion) for this glasses system. Activation energy (E_a) was found to decrease as Sm_2O_3 content increased up to BTS4 due to the samarium oxide substance that modifies the transition state to lower the activation energy.

The optical band gap values have been determined and both direct and indirect transitions are involved, in which both values decreasing with increase of Sm_2O_3 content up to BTS4. So, due to light doping of Sm^{3+} impurity ions, the band tailing (Urbach Energy, ΔE) or impurity band becomes broader and finally reaches and merges the bottom of the conduction band causing the decrease of the optical band gap. This

result suggests that with increasing of Sm_2O_3 concentration, the covalent nature of the glass matrix decreases [17, 22 - 24].

ACKNOWLEDGMENT

The author would like to thank the Ministry of Science, Technology and Innovation, Malaysia (MOSTI) for the fund under Fundamental Research Grant Scheme (FGRS), grant vote 5523752.

REFERENCES

[1] Ni Yaru, Lu Chunhua, Zhang Yan, Zhang Qitu, Xu Zhongzi, *Journal of Rare Earths*, **25**, Suppl., Jun. (2007), 94-98
[2] P. Bergo, W.M. Pontuschka, J.M. Prison, *Journal of Materials Chemistry and Physics* **108**, (2008) 142–146
[3] M.A.K. El-Fayoumi, M. Farouk, *Journal of Alloys and Compounds* **482** (2009) 356-360
[4] S. Rada, M. Culea, E. Culea, *Journal of Non-Crystalline Solids* **354** (2008) 5491-5495
[5] Yasseer B. Saddeek, H.A. Afifi, N.S. Abd El-Aal, *Physica B* **398** (2007) 1-7
[6] Y.C. Ratnakaram, D. Thirupathi Naidu, A. Vijaya Kumar, N.O. Gopal, *Physica B* **358** (2005) 296–307
[7] Akshaya Kumar, D.K. Rai, S.B. Rai, *Spectrochimica Acta Part A,* **59** (2003) 917-925
[8] A.V. Ravi Kumar, B Apparao and N Veeraiah, *Journal of Materials Science,* **21** (4) (1998) 341-347
[9] Lu Chunhua, Ni Yaru, Zhang Qitu, Xu Zhongzi, *Journal of Rare Earths,* **24** (2006) 413-417
[10] R. Van Deun, K. Binnemans, C. Gorller-Walrand and J.L. Adam, "Spectroscopic properties of trivalent Samarium ions in glasses," Celestijnenlaan 200F, B-3001 Heverlee, Belgium, 175-181.
[11] M. Prashant Kumar, T. Sankarappa, B. Vijaya Kumar, N. Nagaraja, *Journal of Solid State Sciences,* **11** (2009) 214–218
[12] M.A. Khaled, H. Elzahed, S.A. Fayek and M.M. El-Ocker, *Journal of Materials Chemistry and Physics,* **37** (1994) 329-332
[13] A.I. Sabry, M. M. El-Samanoudy, *Journal of Materials Science* **30** (1995) 3930-3935
[14] V.Kozhukharov , S.Nikolov , M.Marinov, *Journal of Mat. Res. Bull.* **14** (1979) 735-741
[15] Asst. Prof K.S. Mahesh Lohith, "Dielectric and Magnetics properties of Solids," S B M Jain College of Engineering, Centre for Emerging Technologies.
[16] B.P. Das, P.K. Mahapatra, *Journals of Materials Science: Materials in Electronics* **15** (2004) 107-114
[17] Halimah M.K., Daud W.M., Sidek H.A. A., Zainal A.T., Zainul H. and Jumiah Hassan, *American Journal of Applied Sciences (Special Issue):* 2005, 63-66
[18] Yasser B. Saddeek, Lamia. Abd El Latif, *Physica B* **348** (2004) 475-484

[19] Gorur G. Raju, "Dielectrics in electric field," (Marcel Dekker, Inc, New York, 2003), 163-170.
[20] Robert M. Hill, Colin Pickup, *Journal of Materials Scie*nce, **20** (1985) 4431-4444
[21] Raouf El-Mallawany, *Journal of Materials Chemistry and Physics,* **60** (1999) 103-131
[22] Yanling Wang, Shixun Dai, Feifei Chen, Tiefeng Xu, Qiuhua Nie, *Journal of Materials Chemistry and Physics,* **113** (2009) 407–411
[23] G. Vijaya Prakash, D. Narayana Rao, A.K. Bhatnagar, *Journal of Solid State Communications,* **119** (2001) 39-44
[24] A.A. Dakhel, *Journal of Alloys and Compounds,* **475** (2009) 51-54